www.sciencemag.org/cgi/content/full/science.aad6204/DC1

Supplementary Materials for

Allele-specific inhibitors inactivate mutant KRAS G12C by a trapping mechanism

Piro Lito,* Martha Solomon, Lian-Sheng Li, Rasmus Hansen, Neal Rosen*

*Corresponding author. E-mail: rosenn@mskcc.org (N.R.); litop@mskcc.org (P.L.)

Published 14 January 2016 on *Science* First Release
DOI: 10.1126/science.aad6204

This PDF file includes:

Materials and Methods
Figs. S1 to S7
References

Materials and Methods

Cell culture and reagents

All the cell lines used in this study were obtained from ATCC. The cells were maintained in DMEM medium supplemented with 10% fetal bovine serum, L glutamate, penicillin and streptomycin. ARS853 was obtained from Wellspring Biosciences, AZD8055 and gefitinib from AstraZeneca, while the other inhibitors were obtained from Selleckem. The concentration of ARS853 varied as indicated in the text. The other inhibitor were used at concentrations: gefitinib, 1μM; crizotinib, 1μM; MK2206, 2μM; PD172974, 1μM; afatinib, 1μM; saracatinib, 1μM; BAY806946, 50 nM; trametinib, 50 nM; SCH984, 500 nM and AZD8055, 500 nM.

Cell viability and apoptotic assays

Cells were grown in the presence or absence of inhibitor for various times. Viable cells were determined by using the ATP glow assay as described previously (34). Apoptosis was determined by using staining with annexin V (Invitrogen) according to the manufacturer's protocol. In brief, control or inhibitor-treated cells were harvested and washed in PBS and resuspended in 100 μL of annexin-binding buffer (10 mM HEPES, 140 mM NaCl, and 2.5 mM CaCl2, pH 7.4), followed by addition of 5 μL annexin V and a 15 min incubation at room temperature. Propidium iodide staining was used as a ded cell indicator. After the incubation period 400 μL of annexin-binding buffer was added to the solution followed by FACS analysis. Caspase activity was measured by using the EnzChek caspase assay kit (Invitrogen, E13183), which utilizes Z-DEVD-AMC as a substrate. In brief, control or treated cells were harvested in PBS. The pellets were lysed in lysis buffer provided by the manufacturer. Lysates (50 μg) were loaded in triplicate wells of a 96-well plate and mixed with a substrate working solution and Z-DEVD-AMC substrate as directed by the manufacturer. The samples were incubated at room temperature for 30 min. Caspase activity was assessed by the change in fluorescence (excitation/emission ~342/441 nm) measured in a standard laboratory spectrophotometer.

Proteins for in vitro analyses

The desired HA tagged KRAS mutant constructs were expressed in HEK293 cells (2 μg of plasmid DNA per 60 mm dish). Transfections were performed by using the Lipofectomine 2000 reagent (Invitrogen) according to the manufacturer's recommendations. After 24 hrs the cells were lysed and extracts (1-2 mg) were subjected to affinity purification with a HA-specific antibody resin (Sigma) for 3h or overnight for enzymatic assays or co-IP studies, respectively. The samples were then washed 3-6 times with NP40 lysis buffer. For enzymatic analysis the precipitated fraction was eluted from the resin by using a concentrated HA peptide (Sigma), according to the manufacturer's protocol.

RAS binding domain pull down

These were performed as described previously (35), by using the RAS activation kit from Thermo Scientific (cat. #16117). Briefly, whole cell lysates were incubated with GST-RBD and glutathione beads for 1h followed by three washes in NP40 lysis buffer and elution of pull down fraction with SDS PAGE loading dye. The samples were then

subjected to western blotting with a KRAS specific antibody. When HA-KRAS^{G12C} was exogenously expressed, immunoblotting pull down samples with a HA-specific antibody allowed the specific determination of the levels of mutant KRAS G12C allele in its GTP-bound conformation.

Nucleotide loading of KRAS variants and binding with ARS853

Purified KRAS (1 μM) was incubated EDTA (10 mM) and GDP (1mM) or GTPγS (1mM) at room temperature for 1h followed by addition of MgCl2 (1 mM) to terminate the reaction. Then, ARS853 (1 μM) was then added and the mixture was incubated for another hour at room temperature as described in (8).

Differential scanning fluorimetry

This was performed with the dye kit provided by Invitrogen (cat. # 4461146), exactly as described by the manufacturer. The KRAS samples prepared above were added to thermal shift buffer, fluorescent dye and water and aliquots were placed in the wells of a 394-well plate. The plate was centrifuged at 1000 rpm for 1 min and then loaded into a ViiA7 real time PCR system to perform a melt curve experiment. The temperature was set to escalate on a continuous mode from 25O to 99O at a rate of 1.6O/s and the florescence determined by the ROX reporter with excitation and emission wavelengths of 580±10 and 623±14 respectively. The data were then exported into prism, where the fluorescence signal was plotted as a function of temperature.

In vitro hydrolysis reaction

KRAS proteins, prepared as described above, were eluted in hydrolysis buffer (HEPES pH 7.5, 40 mM, NaCl, 100 mM, MgCl2, 10 mM, DTT, 1 mM, EDTA 2 mM) and mixed with GTP (100 mM) followed by incubation at 37O for 8h, as described previously (18). The released inorganic phosphate was measured by the Cytophos reagent (Cytoskeleton, cat. # BK054) according to the manufacturer recommendations.

KRAS^{G12C}-ARS853 cellular interaction

HEK293 cells expressing various KRAS mutants were treated with compound as indicated. Proteins were extracted using a buffer containing 9M urea, 10 mM DTT and 50 mM ammonium bicarbonate, pH 8, heated to 65ºC for 15 min and alkylated using 50 mM iodoacetamide at 37 ºC for 30 min. The samples were desalted by gel filtration in Zeba™ spin desalting plates (Thermo#89807) followed by addition of sequencing-grade trypsin to a concentration of 10 μg/ml, and incubation for one hour at 37ºC. Heavy isotopic standards (25 fmol) of the KRASG12C target peptide and KRAS normalization peptide were added to the samples followed by desalting in Strata-X polymeric reverse phase plates (Phenomenex #8E-S100-AGB). LC-MS/MS analysis was performed in a Q Exactive™ quadrupole orbitrap mass spectrometer (Thermo Scientific) under standard condition. The amount of KRASG12C bound by the drug was determined by the ratio of the modified G12C peptide to that of the heavy isotopic standards.

KRAS-SOS interaction

This was modified from a previously described protocol (24). HA-tagged KRAS variants were immunoprecipitated with anti HA resin from 1.5 mg of whole cell lysates as

described above. After the final wash, the samples were mixed with recombinant SOS catalytic domain (Cytoskeleton) in binding buffer (20 mM Tris pH7.5, 50 mM NaCl, 1 mM dithiothreitol, 5 mM EDTA and 1%Triton X-100) and incubated for 1 hr at 4O. The samples were then centrifuged at 6,000 rpm, washed several times in binding buffer and KRAS-SOS complexes were eluted in SDS-PAGE loading buffer.

SOS knockdown

Short interfering RNAs targeting SOS1 were obtained from Dharmacon (cat. # L005194), as a pool of four SOS1-specific siRNAs. Cells were transfected with scrambled or SOS1 targeting siRNA pools by using the RNAi reagent (Invitrogen), as directed by the manufacturer.

Synthesis of ARS853

ARS853 or 1-(3-(4-((4-chloro-2-hydroxy-5-(1-methylcyclopropyl)xphenyl)glycyl) piperazin-1-yl)azetidin-1-yl)prop-2-en-1-one was synthesized by Lian-Sheng Li and colleagues at Wellspring Biosciences as first published by Patricelli et al. (11). Synthesis details are repeated here for the reader's convenience.

Acetyl chloride was added to a mixture of methyl 5-amino-2-chloro-4-methoxybenzoate, Et3N and DCM at room temperature and stirred for 12h. The mixture was then partitioned in dichloromethane and water, and the organic layer was washed with NaHCO3 and brine, dried over anhydrous Na2SO4 and concentrated in vacuo. The residue was purified by flash column chromatography on silica gel (ethyl acetate:petroleum ether 1:1) to generate methyl 5-acetamido-2-chloro-4-methoxybenzoate.

Methylmagnesium bromide was added to a solution of methyl 5-acetamido-2-chloro-4-methoxybenzoate in THF under Argon at - 40oC. The mixture was stirred for 2h while allowed to warm to room temperature. The reaction mixture was poured into ice-cooled NH4Cl solution, and extracted with ethyl acetate. The combined organic layer was washed with water and brine, dried over anhydrous Na2SO4 and concentrated in vacuo to yield N-(4-Chloro-5-(2-hydroxypropan-2-yl)-2-methoxyphenyl)acetamide.

SOCl2 was added to a solution of N-(4-chloro-5-(2-hydroxypropan-2-yl)-2-methoxyphenyl) acetamide in DCM at - 5oC. The mixture was warmed to room temperature, and stirred for 2 h. The reaction mixture was concentrated and the residue was purified by flash column chromatography on silica gel to produce N-(4-Chloro-2-methoxy-5-(prop-1-en-2-yl)phenyl)acetamide.

CH2I2 and Et2Zn were added to a solution of N-(4-chloro-2-methoxy-5-(prop-1-en-2-yl)phenyl)acetamide in toluene at 0oC. The mixture was kept at 0oC for 30 min, and then stirred at room temperature for 16 h. The reaction mixture was quenched by stirring in NH4Cl solution for 15 min. The mixture was concentrated in vacuo to remove toluene and the resulting mixture was extracted with dichloromethane. The organic layer was washed with water and brine, dried over anhydrous Na2SO4, and concentrated in vacuo to generate N-(4-Chloro-2-methoxy-5-(1-methylcyclopropyl)phenyl)acetamide.

A mixture of N-(4-chloro-2-methoxy-5-(1-methylcyclopropyl)phenyl)acetamide, KOH, ethanol and water was stirred at reflux for 12 h. The reaction mixture was extracted with

ethyl acetate. The combined organic layer was washed with water and brine, dried over anhydrous Na2SO4, filtered, concentrated in vacuo and then purified by flash column chromatography on silica gel (ethyl acetate:petroleum ether 20:1) to establish 4-chloro-2-methoxy-5-(1-methylcyclopropyl)aniline.

AcOH and ethyl glyoxalate were added to a solution of 4-chloro-2-methoxy-5-(1-methylcyclopropyl)aniline in MeOH at room temperature followed by stirring at room temperature for 2 h. Sodium cyanoborohydride was added followed by stirring at 50°C for 16 h. After cooling to room temperature, the mixture was partitioned in ethyl acetate and water. The organic layer was dried over MgSO4, filtered, and concentrated in vacuo to produce ethyl 2-((4-chloro-2-methoxy-5-(1-methylcyclopropyl)phenyl)amino)acetate:.

LiOH.H2O was added to a solution of ethyl 2-((4-chloro-2-methoxy-5-(1-methylcyclopropyl) phenyl)amino)acetate in THF and water and stirred at room temperature for 2 h. The mixture was washed with ethyl acetate/petroleum ether. The aqueous layer was acidified with aqueous HCl to adjust pH to 3-4 and extracted with ethyl acetate. The organic layer was dried over MgSO4, filtered and concentrated in vacuo to yield 2-((4-Chloro-2-methoxy-5-(1-methylcyclopropyl)phenyl)amino)acetic acid.

BOP and DIEA were added to a solution of 2-((4-chloro-2-methoxy-5-(1-methylcyclopropyl)phenyl)amino)acetic acid and tert-butyl 3-(piperazin-1-yl)azetidine-1-carboxylate in DMF and stirred at room temperature for 1 h. The mixture was partitioned in ethyl acetate and water and the organic layer was washed with brine, dried over MgSO4, filtered and concentrated in vacuo to generate tert-Butyl 3-(4-(2-((4-chloro-2-methoxy-5-(1-methylcyclopropyl)phenyl)amino)acetyl)pi-perazin-1-yl)azetidine-1-carboxylate.

A mixture of tert-butyl 3-(4-(2-((4-chloro-2-methoxy-5-(1-methylcyclopropyl)phenyl) amino)acetyl)piperazin-1-yl)azetidine-1-car-boxylate in HCl-MeOH was stirred at room temperature for 1 h. It was then concentrated in vacuo and the product was mixed for 5 min with Et3N in DCM followed by addition of DMF and acryloyl chloride. The mixture was stirred at room temperature for 1 h, poured into water and then extracted with MeOH/DCM. The organic layer was washed with brine, dried over Na2SO4, concentrated and purified by flash column chromatography on silica gel (DCM:MeOH:NH3.H2O 50:1:0.1 to 20:1:0.2) to generate 1-(3-(4-(2-((4-Chloro-2-hydroxy-5-(1-methylcyclopropyl)phenyl)amino)acetyl)piperazin-1-yl)azetidin-1-yl)prop-2-en-1-one (ARS-853).

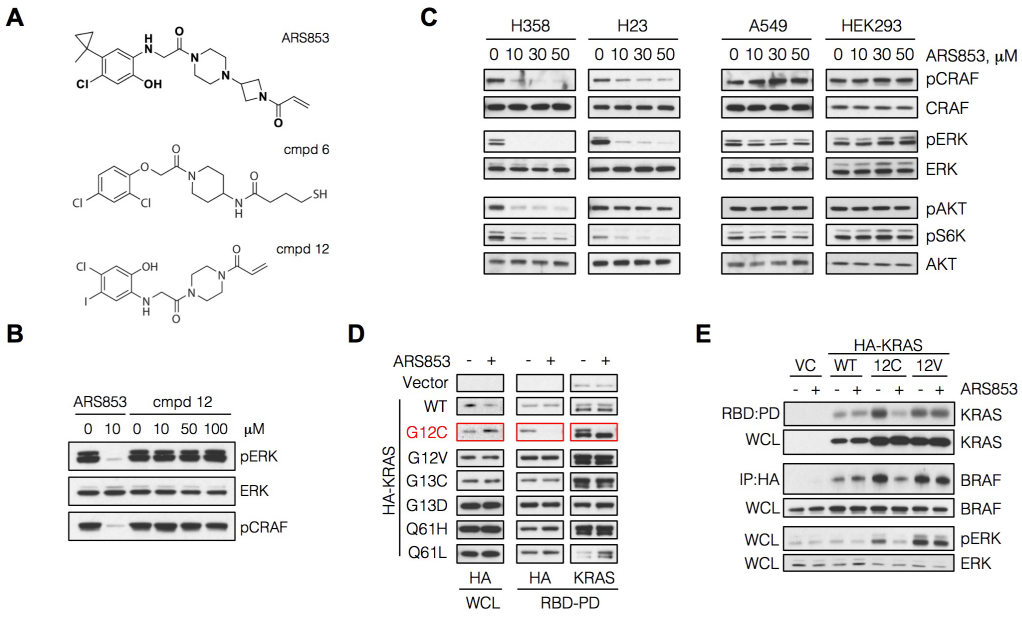

Fig. S1.

ARS853 is an allele-specific inhibitor of KRAS^{G12C}. (**A**) The structure of ARS853 and those of previously reported cmpd 6 and cmpd 12. (**B**) H358 cells treated as shown were evaluated by western blotting to determine the effect on ERK signaling. (**C**) KRAS^{G12C} mutant (H358, H23), KRAS^{G12S} (A549) or KRAS^{WT} (HEK293) cell lines were treated with increasing concentrations of ARS853 to determine the effect on the signaling intermediates shown. (**D**) HEK293 cells were stably transfected with HA-tagged KRAS constructs followed by treatment with ARS853 (10 μM) for 5h. Cell extracts were subjected to a RBD pull-down assay followed by immunoblotting with HA or KRAS-specific antibodies to determine the levels of GTP-bound exogenous KRAS^{G12C} (anti-HA) or endogenous KRAS^{WT} (anti-KRAS, lower band). (**E**) HEK293 cells stably expressing WT, G12C or G12V mutant KRAS were treated and evaluated as in D. In addition they were subjected to an immunoprecipitation reaction with a HA-specific antibody followed by immunoblotting for BRAF to determine the effect on KRAS-BRAF interaction. The effect on ERK phosphorylation is also shown.

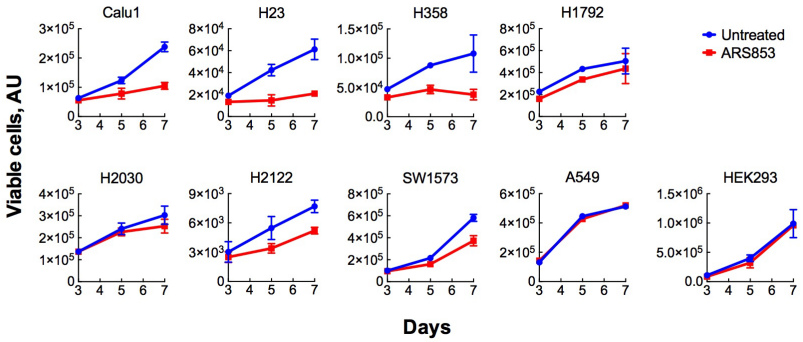

Fig. S2

ARS853 inhibits proliferation in several KRAS^{G12C} mutant lung cancer cells. The indicated cell lines were grown in the presence or absence of ARS853 (10 μM). The number of viable cells was determined using the ATP glow assay (n = 3, mean and s.e.m is shown). A549 cells harbor a KRAS^{G12S} mutation, HEK293 cells harbor KRAS^{WT} alleles and the rest of the cell lines harbor a KRAS^{G12C} mutation.

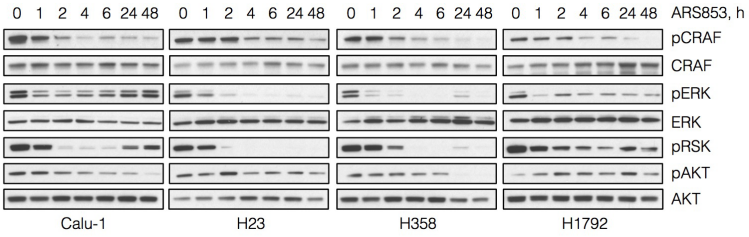

Fig. S3

Inhibition of effector signaling by ARS853 occurs progressively over time. The indicated $KRAS^{G12C}$ cell lines were treated with ARS853 (10 μM) over the times shown to determine the effect on ERK and AKT signaling intermediates. Note the progressive inhibition of CRAF phosphorylation at S338, a site reported to be a marker of RAS-dependent RAF activation (*36*). This correlates with the changes in KRAS-GTP observed in Fig. 2a. The reactivation of ERK or RSK phosphorylation that occurs over time in some cell lines is likely due to compensatory changes in feedback factors.

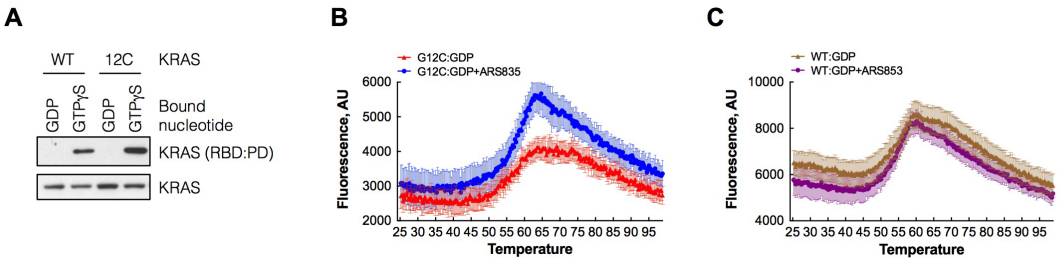

Fig. S4

ARS853 interacts preferentially with GDP-bound KRAS^{G12C}. (**A**) Recombinant KRAS proteins were loaded with GDP or GTPγS followed by an RBD:PD assay to determine the effect of nucleotide loading on the level of active KRAS. (**B**, **C**) The indicated KRAS variants loaded with GDP were reacted with ARS853 and subjected to differential scanning fluorimetry to determine the effect of ARS853 on the thermal denaturation of KRAS (n=4, mean +/- s.e.m.).

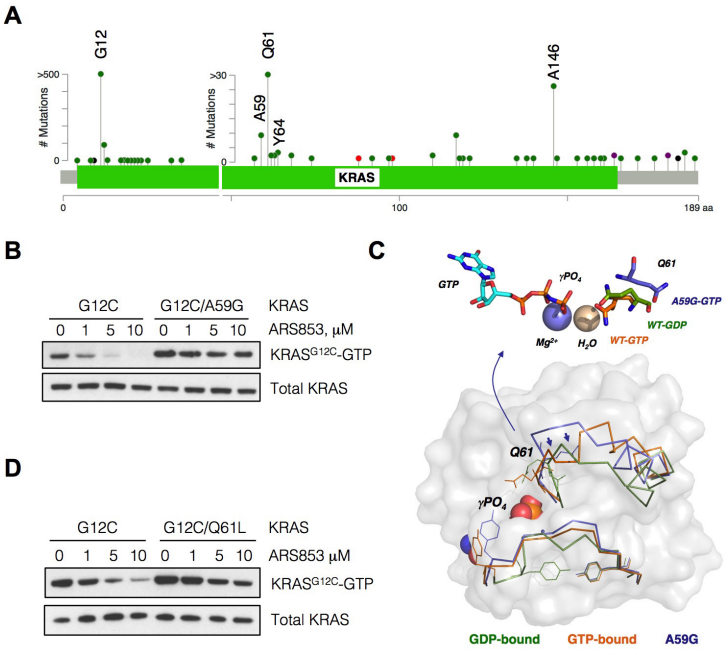

Fig. S5

Impairing the GTPase activity of KRAS^{G12C} attenuates the effect of ARS853. (**A**) Schematic of KRAS mutations found in cancer patients including those used to disrupt or modulate the nucleotide cycle of KRAS^{G12C}. The data were obtained from the 'cBioportal for cancer genomics' database. (**B**) H358 cells expressing the constructs shown were treated with ARS853 for 5h and evaluated by the RBD:PD assay to determine the effect on GTP-bound KRAS^{G12C}. (**C**) The crystal structure of the HRAS A59G mutant (PDB 1lf0) superimposed to the GDP- (PDB 4q21) or GTP- (PDB 4p21) bound structures of HRAS^{WT}. Arrows designate the displacement of Q61 from the γ-phosphate in the A59G mutant. On the top are shown the orientations of the catalytic Q61 residue in wild type (WT) RAS bound to GTP or GDP as well as its orientation in the A59G mutant bound to GTP. The role of Q61 is to coordinate the water molecule involved in the nucleophilic attack of the γ phosphate of GTP. (**D**) HEK293 cells were transfected with the indicated constructs and analyzed as in C. A representative of two independent experiments is shown.

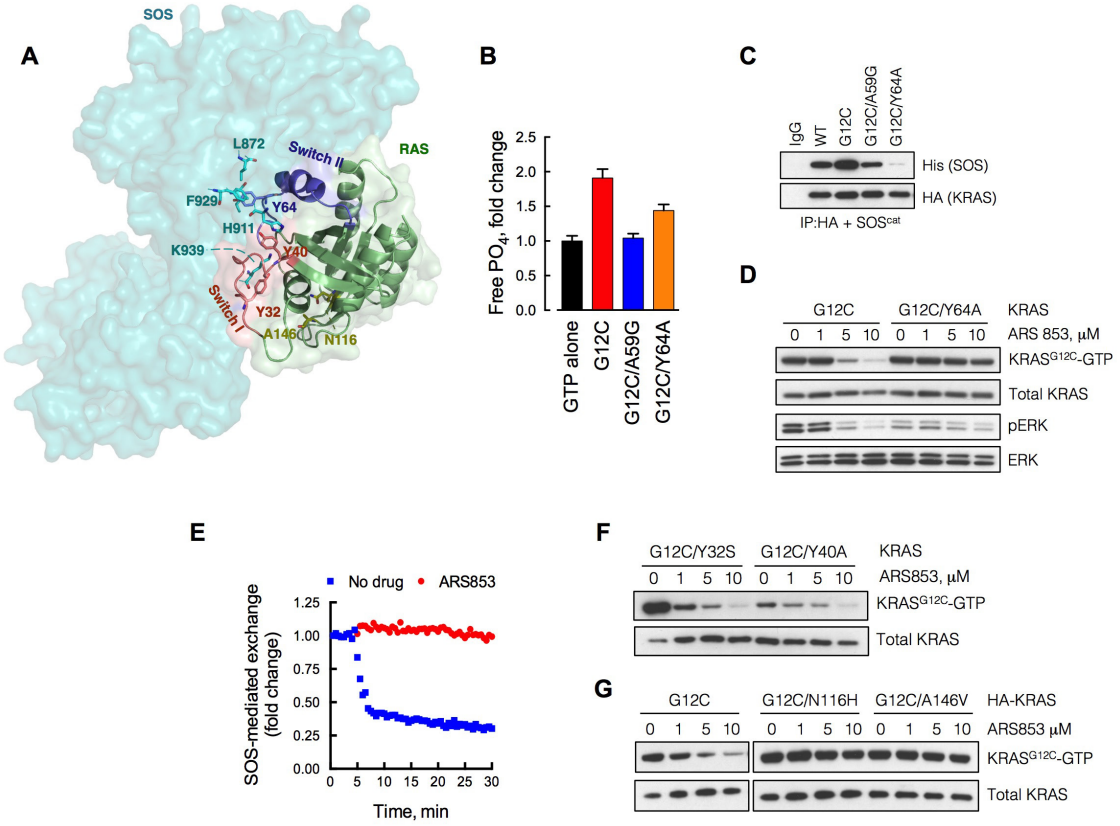

Fig. S6

KRAS^{G12C} inhibition depends on nucleotide exchange activity. (**A**) The crystal structure of nucleotide-free HRAS in complex with SOS (PDB 1bkd). The switch II residue Y64, makes a key hydrophobic interaction with the catalytic (cat) core of SOS. The Y64A mutant has decreased GTPase activity and impaired interaction with SOC^{cat}. The switch I residues Y32 and Y40 are involved in a polar interaction with SOS. Mutations at these residues, i.e. Y32S and Y40A, respectively decrease or increase nucleotide exchange by RAS. Mutations in the two additional residues shown, i.e. N116H and A146V, increase the nucleotide exchange of RAS. (**B**) The KRAS mutants were expressed in HEK293 cells, affinity purified with an anti-HA antibody and then subjected to a GTPase reaction as in Fig. 3B (n=3, mean +/- s.e.m.). (**C**) The KRAS constructs were expressed in HEK293 cells and immunoprecipitation with an anti-HA antibody, followed by a binding assay with purified SOS^{cat}. A representative of two independent experiments is shown. (D) HEK293 cells expressing the indicated constructs were treated with ARS853 for 5h and evaluated to determine the effect on the levels of mutant KRAS-GTP. A representative of three independent experiments is shown. (**E**) Recombinant KRAS^{G12C} was subjected to a nucleotide exchange reaction in the presence of SOS as indicated. (**F**, **G**) H358 (F) or HEK293 (G) cells expressing the indicated mutants were assayed as in D.

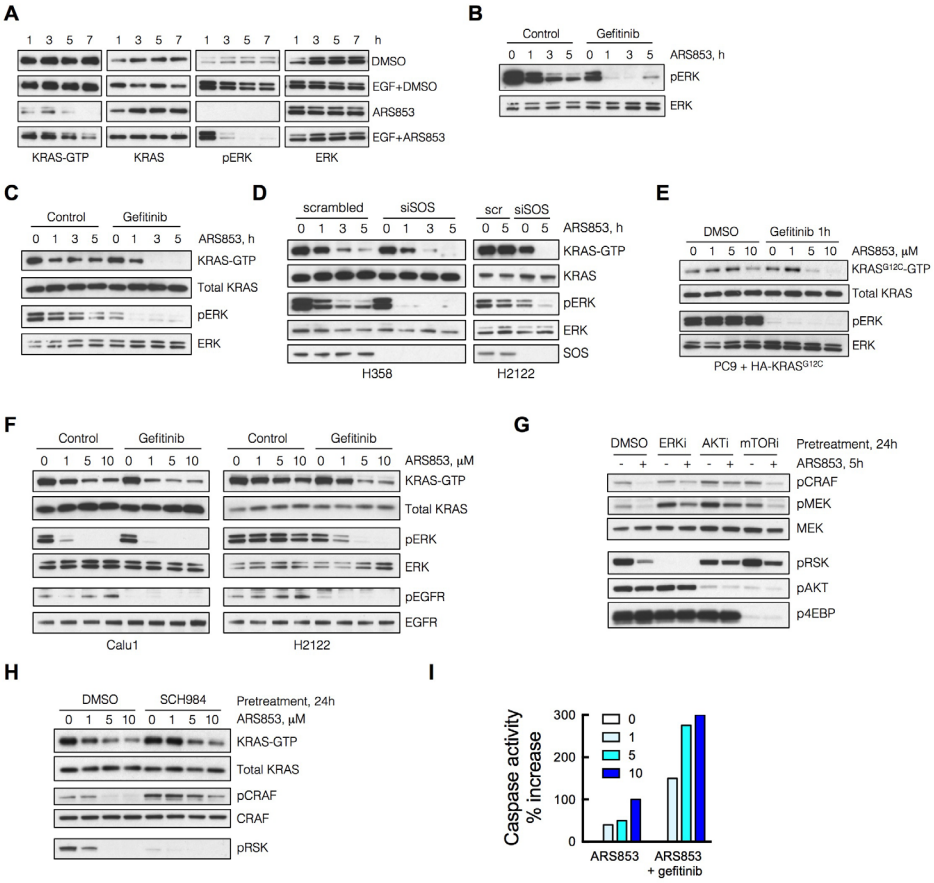

Fig. S7

Nucleotide exchange activity impedes inhibition of KRAS^{G12C} by ARS853. (**A**) Serum deprived KRAS^{G12C} mutant cells were treated with ARS853 with or without EGF to determine the effect on the level of GTP-bound KRAS. (**B, C**) H358 (B) or H2122 (C) cells were treated as shown to determine if EGFR inhibition affects the timing of KRAS^{G12C} inhibition by ARS853. (**D**) The indicated cells were transfected with control or SOS1-specific siRNAs. Four days later they were treated with ARS853 to determine the effect on the inhibition of KRAS^{G12C}. (**E**) HA-tagged KRAS^{G12C} was expressed at a low level in PC9 lung cancer cells (EGFR$^{\Delta ex19}$). Transfected cells were treated with ARS853 in the presence or absence of the EGFR inhibitor gefitinib. The levels of active KRAS^{G12C}-GTP were determined as above. (**F**) KRAS^{G12C}-mutant Calu1 (heterozygous) and H2122 (homozygous) cells were treated with ARS853 in the presence or absence of gefitinib (1 μM) and analyzed to determine the effect on KRAS-GTP and ERK signaling. (**G**, **H**) H358 cells were pre-treated with inhibitors of ERK (SCH984), AKT (MK2206) or mTOR (AZD8055) kinases followed by treatment with ARS853 to determine the effect on CRAF and MEK phosphorylation. The phosphorylation of RSK, AKT, and 4EBP indicates effective inhibition of ERK, AKT, or mTOR, respectively. (**I**) H2122 cells were treated with increasing concentrations of ARS853 (μM), alone or combination with gefitinib. Cell extracts were subjected to a caspase activation assay.

References and Notes

1. Y. Pylayeva-Gupta, E. Grabocka, D. Bar-Sagi, RAS oncogenes: Weaving a tumorigenic web. *Nat. Rev. Cancer* **11**, 761–774 (2011). doi:10.1038/nrc3106 Medline

2. A. G. Stephen, D. Esposito, R. K. Bagni, F. McCormick, Dragging ras back in the ring. *Cancer Cell* **25**, 272–281 (2014). doi:10.1016/j.ccr.2014.02.017 Medline

3. J. L. Bos, H. Rehmann, A. Wittinghofer, GEFs and GAPs: Critical elements in the control of small G proteins. *Cell* **129**, 865–877 (2007). doi:10.1016/j.cell.2007.05.018 Medline

4. L. F. Parada, C. J. Tabin, C. Shih, R. A. Weinberg, Human EJ bladder carcinoma oncogene is homologue of Harvey sarcoma virus ras gene. *Nature* **297**, 474–478 (1982). doi:10.1038/297474a0 Medline

5. E. Santos, S. R. Tronick, S. A. Aaronson, S. Pulciani, M. Barbacid, T24 human bladder carcinoma oncogene is an activated form of the normal human homologue of BALB- and Harvey-MSV transforming genes. *Nature* **298**, 343–347 (1982). doi:10.1038/298343a0 Medline

6. E. Taparowsky, Y. Suard, O. Fasano, K. Shimizu, M. Goldfarb, M. Wigler, Activation of the T24 bladder carcinoma transforming gene is linked to a single amino acid change. *Nature* **300**, 762–765 (1982). doi:10.1038/300762a0 Medline

7. G. Bollag, C. Zhang, Drug discovery: Pocket of opportunity. *Nature* **503**, 475–476 (2013). doi:10.1038/nature12835 Medline

8. A. D. Cox, S. W. Fesik, A. C. Kimmelman, J. Luo, C. J. Der, Drugging the undruggable RAS: Mission possible? *Nat. Rev. Drug Discov.* **13**, 828–851 (2014). doi:10.1038/nrd4389 Medline

9. J. Spiegel, P. M. Cromm, G. Zimmermann, T. N. Grossmann, H. Waldmann, Small-molecule modulation of Ras signaling. *Nat. Chem. Biol.* **10**, 613–622 (2014). doi:10.1038/nchembio.1560 Medline

10. J. M. Ostrem, U. Peters, M. L. Sos, J. A. Wells, K. M. Shokat, K-Ras(G12C) inhibitors allosterically control GTP affinity and effector interactions. *Nature* **503**, 548–551 (2013). doi:10.1038/nature12796 Medline

11. M. P. Patricelli, M. R. Janes, L. S. Li, R. Hansen, U. Peters, L. V. Kessler, Y. Chen, J. M. Kucharski, J. Feng, T. Ely, J. H. Chen, S. J. Firdaus, A. Babbar, P. Ren, Y. Liu, Selective inhibition of oncogenic KRAS output with small molecules targeting the inactive state. *Cancer Discov.* CD-15-1105 (2016). Medline

12. F. H. Niesen, H. Berglund, M. Vedadi, The use of differential scanning fluorimetry to detect ligand interactions that promote protein stability. *Nat. Protoc.* **2**, 2212–2221 (2007). doi:10.1038/nprot.2007.321 Medline

13. S. Gysin, M. Salt, A. Young, F. McCormick, Therapeutic strategies for targeting ras proteins. *Genes Cancer* **2**, 359–372 (2011). doi:10.1177/1947601911412376 Medline

14. G. Bollag, F. McCormick, Differential regulation of rasGAP and neurofibromatosis gene product activities. *Nature* **351**, 576–579 (1991). doi:10.1038/351576a0 Medline

15. K. Scheffzek, M. R. Ahmadian, W. Kabsch, L. Wiesmüller, A. Lautwein, F. Schmitz, A. Wittinghofer, The Ras-RasGAP complex: Structural basis for GTPase activation and its loss in oncogenic Ras mutants. *Science* **277**, 333–338 (1997). doi:10.1126/science.277.5324.333 Medline

16. I. R. Vetter, A. Wittinghofer, The guanine nucleotide-binding switch in three dimensions. *Science* **294**, 1299–1304 (2001). doi:10.1126/science.1062023 Medline

17. B. E. Hall, D. Bar-Sagi, N. Nassar, The structural basis for the transition from Ras-GTP to Ras-GDP. *Proc. Natl. Acad. Sci. U.S.A.* **99**, 12138–12142 (2002). doi:10.1073/pnas.192453199 Medline

18. S. M. Margarit, H. Sondermann, B. E. Hall, B. Nagar, A. Hoelz, M. Pirruccello, D. Bar-Sagi, J. Kuriyan, Structural evidence for feedback activation by Ras.GTP of the Ras-specific nucleotide exchange factor SOS. *Cell* **112**, 685–695 (2003). doi:10.1016/S0092-8674(03)00149-1 Medline

19. M. J. Smith, B. G. Neel, M. Ikura, NMR-based functional profiling of RASopathies and oncogenic RAS mutations. *Proc. Natl. Acad. Sci. U.S.A.* **110**, 4574–4579 (2013). doi:10.1073/pnas.1218173110 Medline

20. P. A. Boriack-Sjodin, S. M. Margarit, D. Bar-Sagi, J. Kuriyan, The structural basis of the activation of Ras by Sos. *Nature* **394**, 337–343 (1998). doi:10.1038/28548 Medline

21. H. Sondermann, S. M. Soisson, S. Boykevisch, S. S. Yang, D. Bar-Sagi, J. Kuriyan, Structural analysis of autoinhibition in the Ras activator Son of sevenless. *Cell* **119**, 393–405 (2004). doi:10.1016/j.cell.2004.10.005 Medline

22. L. A. Feig, G. M. Cooper, Relationship among guanine nucleotide exchange, GTP hydrolysis, and transforming potential of mutated ras proteins. *Mol. Cell. Biol.* **8**, 2472–2478 (1988). doi:10.1128/MCB.8.6.2472 Medline

23. B. E. Hall, S. S. Yang, P. A. Boriack-Sjodin, J. Kuriyan, D. Bar-Sagi, Structure-based mutagenesis reveals distinct functions for Ras switch 1 and switch 2 in Sos-catalyzed guanine nucleotide exchange. *J. Biol. Chem.* **276**, 27629–27637 (2001). doi:10.1074/jbc.M101727200 Medline

24. G. Patel, M. J. MacDonald, R. Khosravi-Far, M. M. Hisaka, C. J. Der, Alternate mechanisms of ras activation are complementary and favor and formation of ras-GTP. *Oncogene* **7**, 283–288 (1992). Medline

25. M. A. Lemmon, J. Schlessinger, Cell signaling by receptor tyrosine kinases. *Cell* **141**, 1117–1134 (2010). doi:10.1016/j.cell.2010.06.011 Medline

26. W. Pao, J. Chmielecki, Rational, biologically based treatment of EGFR-mutant non-small-cell lung cancer. *Nat. Rev. Cancer* **10**, 760–774 (2010). doi:10.1038/nrc2947 Medline

27. T. M. Chin, M. P. Quinlan, A. Singh, L. V. Sequist, T. J. Lynch, D. A. Haber, S. V. Sharma, J. Settleman, Reduced Erlotinib sensitivity of epidermal growth factor receptor-mutant non-small cell lung cancer following cisplatin exposure: A cell culture model of second-line erlotinib treatment. *Clin. Cancer Res.* **14**, 6867–6876 (2008). doi:10.1158/1078-0432.CCR-08-0093 Medline

28. P. Lito, N. Rosen, D. B. Solit, Tumor adaptation and resistance to RAF inhibitors. *Nat. Med.* **19**, 1401–1409 (2013). doi:10.1038/nm.3392 Medline

29. S. Chandarlapaty, A. Sawai, M. Scaltriti, V. Rodrik-Outmezguine, O. Grbovic-Huezo, V. Serra, P. K. Majumder, J. Baselga, N. Rosen, AKT inhibition relieves feedback suppression of receptor tyrosine kinase expression and activity. *Cancer Cell* **19**, 58–71 (2011). doi:10.1016/j.ccr.2010.10.031 Medline

30. P. Lito, C. A. Pratilas, E. W. Joseph, M. Tadi, E. Halilovic, M. Zubrowski, A. Huang, W. L. Wong, M. K. Callahan, T. Merghoub, J. D. Wolchok, E. de Stanchina, S. Chandarlapaty, P. I. Poulikakos, J. A. Fagin, N. Rosen, Relief of profound feedback inhibition of mitogenic signaling by RAF inhibitors attenuates their activity in BRAFV600E melanomas. *Cancer Cell* **22**, 668–682 (2012). doi:10.1016/j.ccr.2012.10.009 Medline

31. C. Navas, I. Hernández-Porras, A. J. Schuhmacher, M. Sibilia, C. Guerra, M. Barbacid, EGF receptor signaling is essential for k-ras oncogene-driven pancreatic ductal adenocarcinoma. *Cancer Cell* **22**, 318–330 (2012). doi:10.1016/j.ccr.2012.08.001 Medline

32. E. A. Collisson, J. D. Campbell, A. N. Brooks, A. H. Berger, W. Lee, J. Chmielecki, D. G. Beer, L. Cope, C. J. Creighton, L. Danilova, L. Ding, G. Getz, P. S. Hammerman, D. Neil Hayes, B. Hernandez, J. G. Herman, J. V. Heymach, I. Jurisica, R. Kucherlapati, D. Kwiatkowski, M. Ladanyi, G. Robertson, N. Schultz, R. Shen, R. Sinha, C. Sougnez, M.-S. Tsao, W. D. Travis, J. N. Weinstein, D. A. Wigle, M. D. Wilkerson, A. Chu, A. D. Cherniack, A. Hadjipanayis, M. Rosenberg, D. J. Weisenberger, P. W. Laird, A. Radenbaugh, S. Ma, J. M. Stuart, L. Averett Byers, S. B. Baylin, R. Govindan, M. Meyerson, M. Rosenberg, S. B. Gabriel, K. Cibulskis, C. Sougnez, J. Kim, C. Stewart, L. Lichtenstein, E. S. Lander, M. S. Lawrence, G. Getz, C. Kandoth, R. Fulton, L. L. Fulton, M. D. McLellan, R. K. Wilson, K. Ye, C. C. Fronick, C. A. Maher, C. A. Miller, M. C. Wendl, C. Cabanski, L. Ding, E. Mardis, R. Govindan, C. J. Creighton, D. Wheeler, M. Balasundaram, Y. S. N. Butterfield, R. Carlsen, A. Chu, E. Chuah, N. Dhalla, R. Guin, C. Hirst, D. Lee, H. I. Li, M. Mayo, R. A. Moore, A. J. Mungall, J. E. Schein, P. Sipahimalani, A. Tam, R. Varhol, A. Gordon Robertson, N. Wye, N. Thiessen, R. A. Holt, S. J. M. Jones, M. A. Marra, J. D. Campbell, A. N. Brooks, J. Chmielecki, M. Imielinski, R. C. Onofrio, E. Hodis, T. Zack, C. Sougnez, E. Helman, C. Sekhar Pedamallu, J. Mesirov, A. D. Cherniack, G. Saksena, S. E. Schumacher, S. L. Carter, B. Hernandez, L. Garraway, R. Beroukhim, S. B. Gabriel, G. Getz, M. Meyerson, A. Hadjipanayis, S. Lee, H. S. Mahadeshwar, A. Pantazi, A. Protopopov, X. Ren, S. Seth, X. Song, J. Tang, L. Yang, J. Zhang, P.-C. Chen, M. Parfenov, A. Wei Xu, N. Santoso, L. Chin, P. J. Park, R. Kucherlapati, K. A. Hoadley, J. Todd Auman, S. Meng, Y. Shi, E. Buda, S. Waring, U. Veluvolu, D. Tan, P. A. Mieczkowski, C. D. Jones, J. V. Simons, M. G. Soloway, T. Bodenheimer, S. R. Jefferys, J. Roach, A. P. Hoyle, J. Wu, S. Balu, D. Singh, J. F. Prins, J. S. Marron, J. S. Parker, D. Neil Hayes, C. M. Perou, J. Liu, L. Cope, L. Danilova, D. J. Weisenberger, D. T. Maglinte, P. H. Lai, M. S. Bootwalla, D. J. Van Den Berg, T. Triche Jr., S. B. Baylin, P. W. Laird, M. Rosenberg, L. Chin, J. Zhang, J. Cho, D. DiCara, D. Heiman, P. Lin, W. Mallard, D. Voet, H. Zhang, L. Zou, M. S. Noble, M. S. Lawrence, G. Saksena, N. Gehlenborg, H. Thorvaldsdottir, J. Mesirov, M.-D. Nazaire, J. Robinson, G. Getz, W. Lee, B. Arman Aksoy, G. Ciriello, B. S. Taylor, G. Dresdner, J. Gao, B. Gross, V. E. Seshan, M. Ladanyi, B. Reva, R. Sinha, S. Onur Sumer,

N. Weinhold, N. Schultz, R. Shen, C. Sander, S. Ng, S. Ma, J. Zhu, A. Radenbaugh, J. M. Stuart, C. C. Benz, C. Yau, D. Haussler, P. T. Spellman, M. D. Wilkerson, J. S. Parker, K. A. Hoadley, P. K. Kimes, D. Neil Hayes, C. M. Perou, B. M. Broom, J. Wang, Y. Lu, P. Kwok Shing Ng, L. Diao, L. Averett Byers, W. Liu, J. V. Heymach, C. I. Amos, J. N. Weinstein, R. Akbani, G. B. Mills, E. Curley, J. Paulauskis, K. Lau, S. Morris, T. Shelton, D. Mallery, J. Gardner, R. Penny, C. Saller, K. Tarvin, W. G. Richards, R. Cerfolio, A. Bryant, D. P. Raymond, N. A. Pennell, C. Farver, C. Czerwinski, L. Huelsenbeck-Dill, M. Iacocca, N. Petrelli, B. Rabeno, J. Brown, T. Bauer, O. Dolzhanskiy, O. Potapova, D. Rotin, O. Voronina, E. Nemirovich-Danchenko, K. V. Fedosenko, A. Gal, M. Behera, S. S. Ramalingam, G. Sica, D. Flieder, J. Boyd, J. E. Weaver, B. Kohl, D. Huy Quoc Thinh, G. Sandusky, H. Juhl, E. Duhig, P. Illei, E. Gabrielson, J. Shin, B. Lee, K. Rogers, D. Trusty, M. V. Brock, C. Williamson, E. Burks, K. Rieger-Christ, A. Holway, T. Sullivan, D. A. Wigle, M. K. Asiedu, F. Kosari, W. D. Travis, N. Rekhtman, M. Zakowski, V. W. Rusch, P. Zippile, J. Suh, H. Pass, C. Goparaju, Y. Owusu-Sarpong, J. M. S. Bartlett, S. Kodeeswaran, J. Parfitt, H. Sekhon, M. Albert, J. Eckman, J. B. Myers, R. Cheney, C. Morrison, C. Gaudioso, J. A. Borgia, P. Bonomi, M. Pool, M. J. Liptay, F. Moiseenko, I. Zaytseva, H. Dienemann, M. Meister, P. A. Schnabel, T. R. Muley, M. Peifer, C. Gomez-Fernandez, L. Herbert, S. Egea, M. Huang, L. B. Thorne, L. Boice, A. Hill Salazar, W. K. Funkhouser, W. Kimryn Rathmell, R. Dhir, S. A. Yousem, S. Dacic, F. Schneider, J. M. Siegfried, R. Hajek, M. A. Watson, S. McDonald, B. Meyers, B. Clarke, I. A. Yang, K. M. Fong, L. Hunter, M. Windsor, R. V. Bowman, S. Peters, I. Letovanec, K. Z. Khan, M. A. Jensen, E. E. Snyder, D. Srinivasan, A. B. Kahn, J. Baboud, D. A. Pot, K. R. Mills Shaw, M. Sheth, T. Davidsen, J. A. Demchok, L. Yang, Z. Wang, R. Tarnuzzer, J. Claude Zenklusen, B. A. Ozenberger, H. J. Sofia, W. D. Travis, R. Cheney, B. Clarke, S. Dacic, E. Duhig, W. K. Funkhouser, P. Illei, C. Farver, N. Rekhtman, G. Sica, J. Suh, M.-S. Tsao; Cancer Genome Atlas Research Network, Comprehensive molecular profiling of lung adenocarcinoma. *Nature* **511**, 543–550 (2014). doi:10.1038/nature13385 Medline

33. P. Rodriguez-Viciana, P. H. Warne, A. Khwaja, B. M. Marte, D. Pappin, P. Das, M. D. Waterfield, A. Ridley, J. Downward, Role of phosphoinositide 3-OH kinase in cell transformation and control of the actin cytoskeleton by Ras. *Cell* **89**, 457–467 (1997). doi:10.1016/S0092-8674(00)80226-3 Medline

34. P. Lito, A. Saborowski, J. Yue, M. Solomon, E. Joseph, S. Gadal, M. Saborowski, E. Kastenhuber, C. Fellmann, K. Ohara, K. Morikami, T. Miura, C. Lukacs, N. Ishii, S. Lowe, N. Rosen, Disruption of CRAF-mediated MEK activation is required for effective MEK inhibition in KRAS mutant tumors. *Cancer Cell* **25**, 697–710 (2014). doi:10.1016/j.ccr.2014.03.011 Medline

35. S. J. Taylor, R. J. Resnick, D. Shalloway, Nonradioactive determination of Ras-GTP levels using activated ras interaction assay. *Methods Enzymol.* **333**, 333–342 (2001). doi:10.1016/S0076-6879(01)33067-7 Medline

36. C. S. Mason, C. J. Springer, R. G. Cooper, G. Superti-Furga, C. J. Marshall, R. Marais, Serine and tyrosine phosphorylations cooperate in Raf-1, but not B-Raf activation. *EMBO J.* **18**, 2137–2148 (1999). doi:10.1093/emboj/18.8.2137 Medline